

¹³C NMR studies of the binding of medium-chain fatty acids to human serum albumin

Marie A. Kenyon and James A. Hamilton¹

Department of Biophysics, Housman Research Center, Boston University Medical School, 80 E. Concord Street, R111, Boston, MA 02118-2394

Abstract Binding of the medium-chain fatty acids (MCFA), octanoic (OCT) and decanoic (DEC) acid, to human serum albumin (HSA) has been studied by ¹³C NMR spectroscopy. NMR spectra at 35°C showed an apparently homogeneous binding environment (a single, narrow resonance for the ¹³C-enriched carboxyl carbon) at different mole ratios and pH values. Changes in the chemical shift of this peak with mole ratio and protein concentration demonstrated rapid equilibration (\leq msec) of bound and unbound MCFA and permitted a direct quantitation of bound/unbound MCFA. Spectra of OCT/HSA mixtures at 6°C revealed at least three distinct binding sites that fill sequentially. The observed heterogeneity of binding at low temperature, compared to 35°C, is attributed to a slower exchange rate of OCT between binding sites. The highest affinity sites for both OCT and DEC have properties similar to those of binding sites for longer-chain fatty acids, such as the close proximity of the fatty acid carboxylate to basic amino acid residue(s). Interestingly, chemical shift data showed that the first mole of OCT and DEC either bind differently to the same site or bind to different sites on HSA. The rapid desorption of MCFA from HSA binding sites has implications for dietary regimens with medium chain triglycerols.—Kenyon, M. A., and J. A. Hamilton. ¹³C NMR studies of the binding of medium-chain fatty acids to human serum albumin. *J. Lipid Res.* 1994. 35: 458-467.

Supplementary key words octanoic acid • decanoic acid • binding affinities • exchange rates • parenteral feeding

Human serum albumin (HSA) is a key transport protein in plasma that plays an important role in lipid metabolism by virtue of its high-affinity and high-capacity binding of free (unesterified) fatty acids (FA). The physiological importance of plasma free FA and the pathological effects resulting from abnormally high levels of free FA (1) have encouraged ongoing investigations of the binding and transport of free FA by albumin. The high-resolution X-ray structure of FA-free HSA (2) shows elegantly and in great detail the loops and domains that were predicted by numerous investigators (3). Nevertheless, molecular details of the binding of FA, particularly those of medium-chain length (8 or 10 carbons), are incomplete. Although medium-chain fatty acids (MCFA) normally constitute a very minor fraction of the FA in plasma, interest in the

binding of MCFA exists as the levels of these FA can be greatly elevated in certain disease states (4), in patients fed intravenous medium chain triacylglycerols (4-6) and in infants treated for low birth weight (7). Interest in the binding of MCFA to HSA also stems from the observation that these acids may compete with certain drugs and with tryptophan for binding sites on HSA (8-11).

Interactions of MCFA with albumin have previously been probed by analysis of equilibrium binding data in the presence and absence of competing ligands (9, 12) and as a function of pH (12). However, equilibrium binding studies do not differentiate multiple binding sites with similar affinities and do not provide direct information about structural features of the binding sites. Additional strategies have attempted to locate MCFA binding sites on serum albumin by covalent modification of HSA (13) and by fragments of bovine serum albumin (BSA) (14, 15).

A more recent approach for examining interactions of FA with albumin has been ¹³C NMR spectroscopy. This spectroscopic approach, which uses native FA with a non-perturbing modification (¹³C enrichment), can provide information about molecular interactions in individual binding sites, in contrast to methods that report on average behavior. New information has been provided about ionic interactions between the FA carboxyl group and the amino acids in the binding sites on BSA, about the location of high affinity sites on BSA for long-chain fatty acids, and about the dependence of interactions on FA chain length (16-20). Like classical approaches, ¹³C NMR spectroscopy has provided less information about the binding of MCFA to albumin (21) than about long-chain FA and, to date, most studies have focused on BSA rather than HSA. In this study, interactions of MCFA [OCT (8 carbon) and DEC (10 car-

Abbreviations: MCFA, medium-chain fatty acids; HSA, human serum albumin; FA, fatty acid; OCT, octanoic acid; DEC, decanoic acid; BSA, bovine serum albumin; CD, circular dichroism; UV, ultraviolet; TMS, tetramethylsilane.

¹To whom correspondence should be addressed.

bon]] with HSA were investigated by high-resolution ^{13}C NMR spectroscopy. NMR measurements (primarily chemical shift and lineshape) were made as a function of pH, temperature, and the mole ratio of FA to albumin. Our results illuminate molecular aspects of MCFA binding to HSA.

MATERIALS AND METHODS

Materials

Lyophilized, crystallized HSA (A3782, primarily Lot 127F-9310) was obtained from Sigma Chemical Co., St. Louis, MO. The essentially FA-free HSA contained less than 0.01 mole of FA per mole of protein as determined by gas-liquid chromatography. Ninety percent ^{13}C carboxyl-enriched OCT and DEC used in this study were purchased from CIL, Cambridge, MA.

Sample preparation

A measured amount of HSA was dissolved in 0.56% KCl and the protein concentration was determined from the absorbance at 279 nm (22) of filtered 1:100 dilutions in 7.5 mM KCl; the extinction coefficient used was $0.55\text{ ml mg}^{-1}\text{cm}^{-1}$ (23). The protein concentration was $\sim 93\text{ mg/ml}$ for all NMR samples unless otherwise stated. OCT/HSA and DEC/HSA complexes were prepared with aqueous potassium OCT and with aqueous potassium DEC, respectively. The concentration of the FA, dissolved in chloroform-methanol 2:1, was determined by measuring dry weights on an electrobalance (Cahn model 25, Cerritos, CA). The aqueous solutions of potassium FA were made by combining a known amount of ^{13}C -enriched FA with 1.2 eq of base (1 N KOH, 0.1 N KOH). Sodium could be substituted for potassium, yielding identical results. FA/HSA samples were made by the addition of an appropriate amount of potassium FA (depending on the desired mole ratio of FA to HSA) directly to a measured volume of aqueous protein (1.4–1.6 ml). To increase the mole ratio, FA was added directly to the FA/HSA complex. OCT/HSA and DEC/HSA mixtures were gently vortexed and these samples were adjusted initially to a pH of 7.4. During the course of some experiments, the pH of the samples was changed by adding small amounts of KOH (0.1 N, 1 N) or HCl (0.1 N, 1 N) directly to the NMR tube, using a microliter syringe. The pH values were measured by a Beckman model 3560 pH meter equipped with a 5-mm diameter microelectrode. pH values for the FA/HSA samples before and after NMR analysis differed by ≤ 0.2 pH units. Final pH values are reported.

^{13}C NMR spectroscopy

A Bruker WP-200 spectrometer operating at 4.7 T (50.3 MHz) was used, unless otherwise noted, to obtain ^{13}C NMR spectra (16). Selected spectra were obtained

with a Bruker AMX 300 spectrometer operating at 7.05 T (75 MHz for ^{13}C). Spectra were obtained with 16K time domain points and a 10 KHz (4.7 T) or 15 KHz (7.05 T) spectral width. Aqueous FA-albumin complexes included $100\text{ }\mu\text{l}$ of D_2O for a lock and a shim signal. The NMR sample tubes supported an insert containing tetramethylsilane (TMS) in CDCl_3 . All chemical shifts were measured with respect to this external reference. The uncertainty of all chemical shift values reported is ± 0.05 ppm, based on multiple measurements of samples with similar compositions prepared and analyzed at different times. Each NMR experiment reported in this study was repeated one to three times. Data shown are representative data. The temperature dependence of the reference signal was estimated to be < 0.1 ppm in the temperature range investigated. Temperature was controlled (± 1 – 2°C) with a Bruker B-VT-1000 variable temperature unit. The internal temperature of selected samples was measured as follows. After the sample had equilibrated in the magnet for ~ 10 min at a fixed temperature that was regulated by the variable control unit, the sample was removed (time zero). A thermocouple was immediately inserted in the sample and several temperature values were recorded at 15-sec intervals. The temperature at time zero (corresponding to the true sample temperature) was obtained by extrapolation of the linear relationship of temperature versus time. A temperature calibration curve was constructed from measurements at several temperatures.

Spin lattice relaxation time was measured for selected samples by the fast inversion-recovery method (24). Pulse intervals for obtaining standard spectra were generally chosen for optimal signal to noise ratios ($\sim 1 \times T_1$) rather than for equilibrium intensities ($5 \times T_1$). Deconvolution of spectra was performed with NMR1 (New Methods Research, Inc., East Syracuse, NY).

CD spectroscopy

Near-UV CD spectra were recorded using a Cary 61 CD spectropolarimeter (Varian, Palo Alto, CA). Three continuous spectra per sample were recorded in the wavelength range of 320–260 nm. Data points were analyzed at 1-nm intervals; trough depth measurements were made with respect to the baseline value. Molar ellipticity values [θ], in units of $\text{deg}\cdot\text{cm}^2/\text{dmol}$, were calculated by the standard equation for a path length of 0.02 cm (25).

For temperature-dependent CD spectra, the sample temperature was maintained by circulating ethylene glycol-water through the lamp compartment by means of a thermostated refrigerator-heater bath (NESLAB, Portsmouth, NH). Temperature was measured to within 0.1°C by means of a copper-constantan thermocouple positioned in contact with the CD cell. With each temperature change CD spectra were recorded after a short time interval (~ 15 min) to allow the sample to equilibrate at the desired temperature setting.

RESULTS

NMR studies at 35°C

^{13}C NMR spectra for mixtures of ^{13}C carboxyl-enriched OCT or DEC with HSA were obtained as a function of mole ratio of FA to protein at $T = 34.5^\circ\text{C}$ and $\text{pH} = 7.40 \pm 0.15$. The MCFA carboxyl carbon gave a single peak at all mole ratios; the intensity of this peak increased relative to that of protein peaks (e.g., the broad carbonyl at $\sim 170\text{--}180$ ppm) with increasing FA to HSA mole ratio. Under similar experimental conditions, FA with a chain length of ≥ 12 carbons in the presence of HSA or BSA give rise to multiple narrow signals whose individual intensities increase with increasing mole ratio (18, 26). For OCT and DEC the chemical shift of the single carboxyl peak showed a dependence on mole ratio (Fig. 1A). For OCT/HSA mixtures, the chemical shift increased steadily with increasing mole ratio of FA/HSA, from 181.80 ppm (1:1 OCT/HSA) to 182.83 ppm (15:1 OCT/HSA). The value of the chemical shift approached but did not reach that of unbound OCT (184.32 ppm; see below). In contrast, the chemical shift of DEC/HSA mixtures showed only a small dependence on mole ratio except at very high ratios (Fig. 1A). Between a 3:1 and 11:1 mole ratio of DEC/HSA, there was a small (0.28 ppm) linear increase in chemical shift. Above 11:1 DEC/HSA, a progressive shift to higher ppm was seen.

The dependence of the FA carboxyl chemical shift on protein concentration was examined at 34.5°C and $\text{pH} = 7.4$ by diluting samples with a fixed mole ratio of OCT or DEC to albumin (3:1 and 10:1) from 90–100 mg protein/ml to the lowest concentration feasible for NMR studies (10–20 mg/ml). In all cases a single, narrow resonance from the FA carboxyl carbon was observed. The FA chemical shift for the OCT/HSA system was more dependent on protein concentration than that of the DEC/HSA system (Fig. 1B). The OCT carboxyl peak shifted downfield (to higher ppm) with decreasing HSA concentration, from 182.05 ppm (92 mg/ml) to 182.50 ppm (23 mg/ml) for a 3:1 OCT/HSA complex and from 182.30 ppm (98 mg/ml) to 183.15 ppm (12 mg/ml) for a 10:1 OCT/HSA complex. The chemical shift for the 3:1 DEC/HSA complex remained constant at 182.20 ppm for all HSA concentrations, whereas the 10:1 DEC/HSA mixture showed a slight increase in chemical shift (from 182.30 ppm to 182.45 ppm) at the lowest concentration (12 mg/ml).

NMR spectra obtained as a function of pH can provide important information about binding interactions from the ionization behavior of FA in the presence of protein (16, 19). Therefore, ^{13}C NMR spectra were obtained at 34.5°C as a function of pH for several mole ratios of OCT/albumin (1.5:1, 3:1, and 5:1). These spectra showed a single resonance under all conditions. Fig. 2 compares the titration behavior of OCT in the presence of HSA (3:1

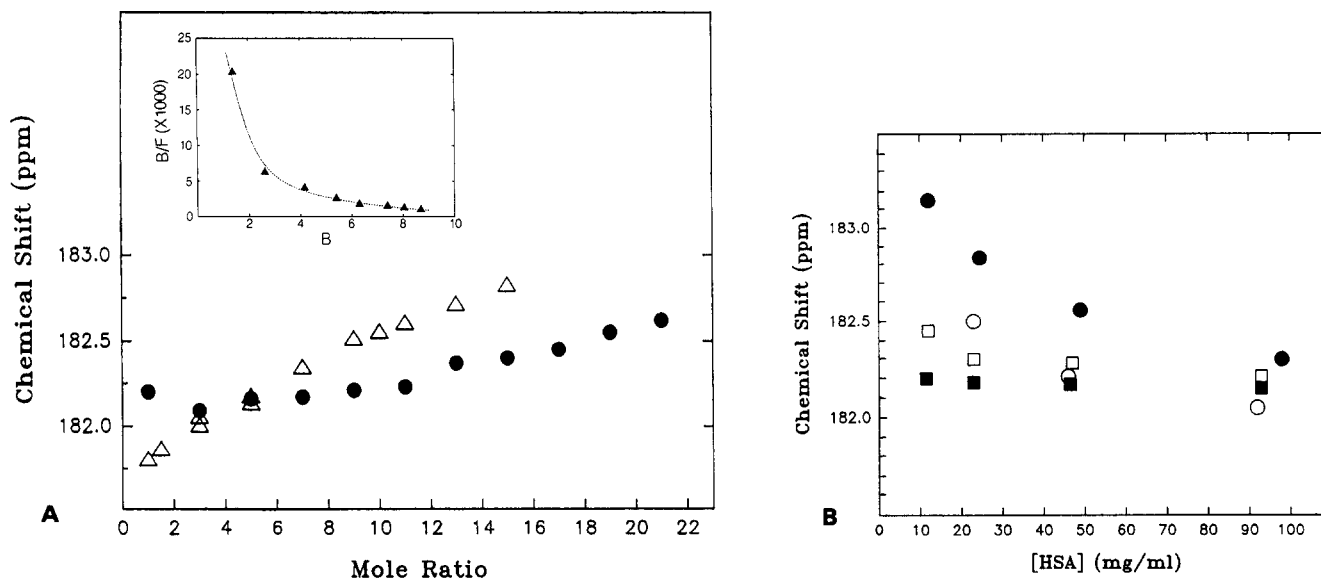


Fig. 1. A: Plot of FA carboxyl ^{13}C chemical shift versus mole ratio at $T = 34.5^\circ\text{C}$ and $\text{pH} = 7.4 \pm 0.2$. The mole ratio represents the stoichiometric amount of FA and albumin in the mixture. Filled circles represent DEC/HSA mixtures; unfilled triangles correspond to OCT/HSA mixtures. All samples had a protein concentration of 93 mg/ml. The inset shows a Scatchard plot of the mole ratio data for a three-term fit. B: Plot of FA carboxyl ^{13}C chemical shift versus HSA concentration at $T = 34.5^\circ\text{C}$ and $\text{pH} = 7.4 \pm 0.2$. Open and closed circles represent 3:1 and 10:1 OCT/HSA mixtures, respectively. Closed and open squares correspond to 3:1 and 10:1 DEC/HSA mixtures, respectively. Conditions for obtaining NMR spectra were as follows: spectral accumulations ranged from 250 to 1000 for DEC/HSA and 6800 to 10,000 for OCT/HSA over 16,384 time domain points with a pulse interval of 2.0 sec. Chemical shift values were measured with respect to an external reference (tetramethylsilane) in units of ppm (parts per million).

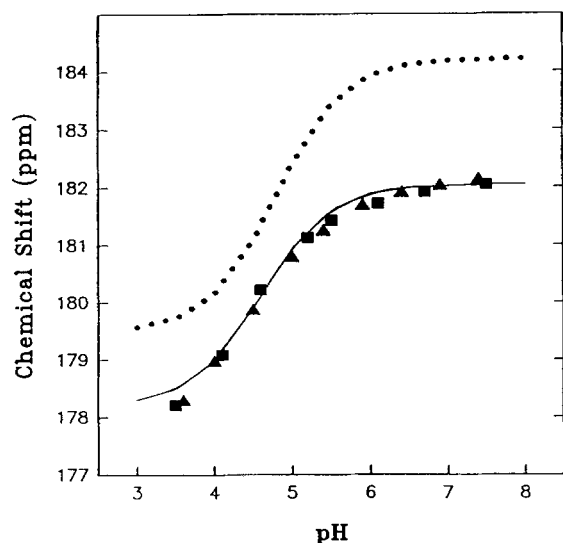


Fig. 2. Plot of OCT carboxyl ^{13}C chemical shift versus pH at $T = 34.5^\circ\text{C}$ and mole ratios of 3:1 (filled square) and 5:1 (filled triangle) OCT/HSA. The protein concentration of all samples was 92–93 mg/ml. The solid line is the theoretically calculated Henderson-Hasselbach curve for a 3:1 OCT/HSA mixture. The dashed curve is the ^{13}C NMR titration of aqueous octanoic acid at 1.6 mM and 40°C (20).

and 5:1 mole ratios) with that of OCT in the absence of protein. The plot of chemical shift versus pH closely follows the sigmoidal Henderson-Hasselbach behavior that is characteristic of an acid–base titration (27). The apparent pK_a value for OCT/HSA complexes was the same as the pK_a of aqueous OCT ($\text{pK}_a = 4.6$). However, the titration curve for OCT with HSA is shifted to lower ppm compared to the curve for unbound OCT, a shift that reflects partitioning of MCFA into a less hydrophilic environment than water (i.e., interactions of OCT with the protein). pH-dependent spectra (not shown) were also obtained at 34.5°C for DEC/HSA complexes at 1.5:1 and 3:1 mole ratios. For the 1.5:1 mole ratio, the chemical shift was monitored between pH 8.1 (182.16 ppm) and pH 6.1 (182.01 ppm), below which the carboxyl signal became too broad to measure the chemical shift. For the 3:1 mole ratio, it was possible to measure the chemical shift at lower pH values. The chemical shift decreased from 182.26 ppm at pH 8.4 to 181.21 ppm at pH 4.7. These data for the 3:1 DEC/HSA complex suggest a titration of DEC similar to that for OCT in the presence of HSA (Fig. 2).

NMR studies at low temperature

In the above NMR studies at 35°C , the FA carboxyl group appeared to experience a single “binding” environment under various experimental conditions: different FA/HSA mole ratios, pH values, and protein concentrations. These results could mean that binding sites for MCFA are not structurally heterogeneous (unlike the case for long-chain FA) or that the NMR experiments did not detect heterogeneous sites. The latter case could occur if

FA in different binding sites exchange rapidly to produce an apparent “single” site, which has been shown to occur with binding of MCFA to BSA (21). As it was possible to detect multiple binding sites for MCFA on BSA at lower temperatures (21), a similar strategy was applied to HSA complexes with OCT and with DEC at fixed mole ratios of MCFA/HSA (1.5:1, 3:1, 5:1) and at $\text{pH } 7.5 \pm 0.1$. Fig. 3 illustrates ^{13}C NMR spectra (FA carboxyl region) for a 3:1 mole ratio complex of OCT/HSA at five temperatures. At the higher temperatures (41.5°C and 34.5°C), a single narrow peak (181.97 ppm and 182.01 ppm, respectively) was observed from the ^{13}C -enriched MCFA. As the temperature was decreased, the carboxyl resonance first broadened (Fig. 3C) and then separated into two major signals (Fig. 3D). At 6.5°C (Fig. 3E) the spectrum exhibited one signal at higher ppm and the other at lower ppm relative to the single signal at 35°C , characteristic of exchange (see below). A spectrum at $\sim 6^\circ$ obtained at 75 MHz (not shown) did not show improved resolution relative to the spectrum at 50 MHz (Fig. 3E).

Temperature-dependent spectra for a 3:1 DEC/HSA

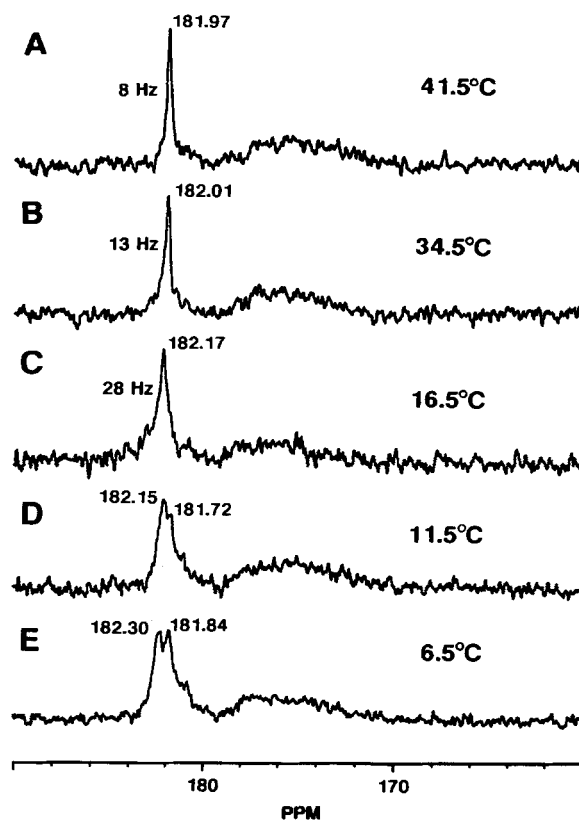


Fig. 3. The carboxyl and carbonyl regions of ^{13}C NMR spectra for a 3:1 mole ratio of 90% $[1-^{13}\text{C}]$ OCT/HSA complex at various temperature values: A) $T = 41.5^\circ\text{C}$ after 1000 accumulations; B) $T = 34.5^\circ\text{C}$ after 1000 accumulations; C) $T = 16.5^\circ\text{C}$ after 4000 accumulations; D) $T = 11.5^\circ\text{C}$ after 8000 accumulations; and E) $T = 6.5^\circ\text{C}$ after 1186 accumulations. All spectra were recorded with a pulse interval of 2.0 sec and processed with a line broadening 4.0 Hz. The sample pH was 7.4 ± 0.1 and the protein concentration was 93 mg/ml.

are shown in **Fig. 4A**. For this mole ratio, as well as the two other mole ratios investigated (1.5 and 5.0), a single carboxyl resonance was observed at $T > 21^\circ\text{C}$ (Fig. 4A, top spectrum). As the temperature was decreased (e.g., 20.5°C), the chemical shift of the predominant peak shifted downfield slightly and a second small signal was seen upfield from this signal (Fig. 4A, middle spectrum). At 6.5°C the major signal was at 182.30 ppm and a broader, less defined signal was seen between 181.64 ppm and 181.15 ppm (Fig. 4A, bottom spectrum). A low temperature spectrum at higher field (75 MHz) showed evidence of a third signal at 181.96 ppm between the two separated peaks (Fig. 4A, right side). The carboxyl spectral region for 1 mole DEC/mole HSA at $T = 6.5^\circ\text{C}$ is shown in Fig. 4B (top spectrum). The spectrum of FA-free HSA (Fig. 4B, bottom spectrum) contains signals around

181.09 ppm from amino acid carboxyl groups that are shifted away from the intense, broad envelope of carbonyl/carboxyl resonances, similar to the case for BSA (16). Subtraction of the protein component from the spectrum for 1:1 DEC/HSA revealed a narrow peak centered at 182.28 ppm (Fig. 4B).

Temperature-dependent spectra in the same temperature range as for OCT and for DEC were obtained for the 12-carbon fatty acids (dodecanoic or lauric). These spectra gave three resonances (181.8, 182.0, and 182.3) for a 3:1 mole ratio of FA/HSA at high temperature, as shown previously (26). There was little effect of temperature in the carboxyl spectrum. Therefore, the temperature-dependent changes described above are specific for MCFAs and are not due to protein aggregation or other general temperature-dependent structural changes.

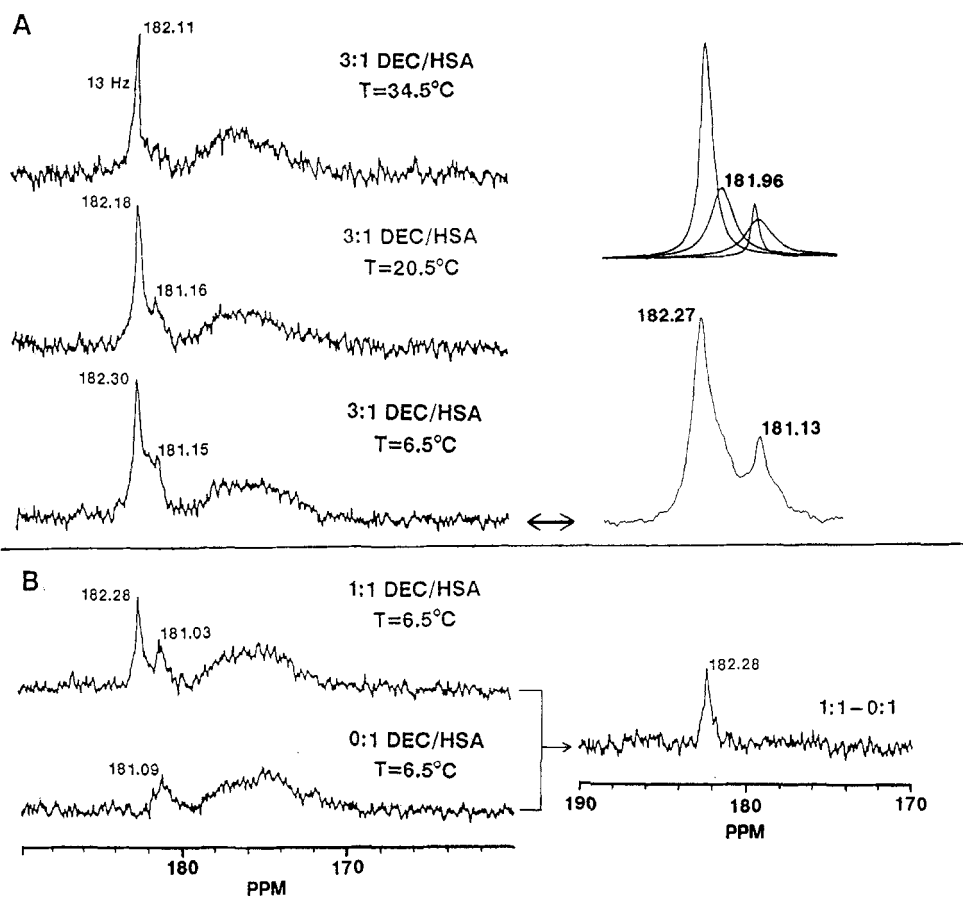


Fig. 4. The carboxyl and carbonyl regions of ^{13}C NMR spectra for A) a 3:1 mole ratio of 90% $[1-^{13}\text{C}]$ DEC/HSA mixture at various temperatures: $T = 34.5^\circ\text{C}$, 1200 scans (top spectrum); $T = 20.5^\circ\text{C}$, 2000 scans (middle spectrum); and $T = 6.5^\circ\text{C}$, 3003 scans (bottom spectrum) and for B) a 1:1 mole ratio of 90% $[1-^{13}\text{C}]$ DEC/HSA sample at 6.5°C , recorded after 4000 scans (top spectrum); a spectrum of FA-free HSA at 6.5°C (bottom spectrum); and the difference of the 1:1 and 0:1 mole ratio of DEC/HSA (right). A spectrum (4000 scans) of a 3:1 DEC/HSA sample at 6.5°C recorded at a higher field (7.05 T) and the corresponding deconvolution spectrum are shown in panel A (right column). The deconvolution shows, in addition to the narrow signals at 182.27 ppm and 181.13 ppm, a broader signal at 181.96 ppm, representing a third binding environment for DEC, and a weaker broad signal from protein carboxylates underlying the FA carboxyl signal at 181.13 ppm (see panel B, bottom spectrum). All other NMR and sample conditions were the same as those stated in Figs. 1 and 3.

Additional NMR studies of OCT binding to HSA were conducted at low temperature ($T = 6.5^\circ\text{C}$) where multiple binding environments were detected. Because the spectrum for 3:1 OCT/HSA showed (at least) two binding environments, it was of interest to examine different mole ratios of OCT to HSA in order to determine whether the sites fill sequentially or simultaneously. **Fig. 5** shows spectra (carboxyl region) for 0, 1, 2, and 3 moles of OCT/mole of HSA. At the lowest mole ratio of OCT studied (1:1 OCT/HSA), a strong carboxyl signal was seen at 181.83 ppm, along with weaker signal(s) at ~ 181.16 ppm (Fig. 5B) that are coincident, or nearly so, with the signal from the protein amino acid carboxylates (Fig. 4B, bottom spectrum; Fig. 5A). The difference spectrum of B-A (Fig. 5E) revealed a single peak at 181.83 ppm which represents the primary binding site for OCT (see below). This chemical shift is the same as that for a 1:1 mole ratio of OCT to HSA at 35°C (Fig. 1). (The temperature insensitivity of this chemical shift was confirmed in a separate experiment in which the same sample (1:1 OCT/HSA) was analyzed at 35°C and 5°C .) With 2 moles of OCT the carboxyl spectrum at 6.5°C showed a peak at 181.83 ppm with a shoulder at 182.14 ppm, representing a new environment (Fig. 5C). The difference spectrum of C-B, which reflects the signal intensity correlated with the addition of a second mole of OCT, showed a single peak at 182.14 ppm (Fig. 5F). Addition of a third mole of OCT to the OCT/HSA mixture yielded a spectrum (Fig. 5D; see also Fig. 3E) with two resonances (181.84 ppm and 182.30 ppm). The difference spectrum, representing the

addition of a third mole of OCT (Fig. 5G), showed a single peak at 182.30 ppm. No additional environments were detected at higher mole ratios of OCT to HSA (spectra not shown). The above results show three major environments represented by signals at 181.8 ppm, 182.1 ppm, and 182.3 ppm and suggest sequential filling of different binding sites whose affinity for OCT differs by ≥ 5 -fold (see discussion).

Using low temperature as a probe of FA-protein interactions, pH-dependent data were obtained to assess structural features of individual binding sites for MCFA on HSA. Spectra of a 3:1 and 5:1 mole ratio of OCT/HSA showed multiple binding sites at various pH values, in contrast to the titration data at 35°C (Fig. 2). Low temperature spectra for a 3:1 mole ratio DEC/HSA sample revealed two resonances (~ 182.3 ppm and ~ 181.2 ppm, as in Fig. 4A) that were both independent of pH (between 5.0 and 8.5).

Fig. 6 shows the NMR titration plot for 3:1 OCT/HSA at low temperature. As there was a signal at 181.8 ppm for all pH values, it was assumed that this represented a peak with an invariant chemical shift. The peak representing the third binding site for OCT (182.3 ppm at pH 7.4) showed a change in chemical shift with pH. The peak for the second mole (182.1 ppm at pH 7.4) was submerged between the other two peaks and apparently did not shift with pH. These titration data suggest stronger ionic interactions between amino acids and OCT in the first (181.8 ppm) and second binding sites (182.1 ppm) than in the third site.

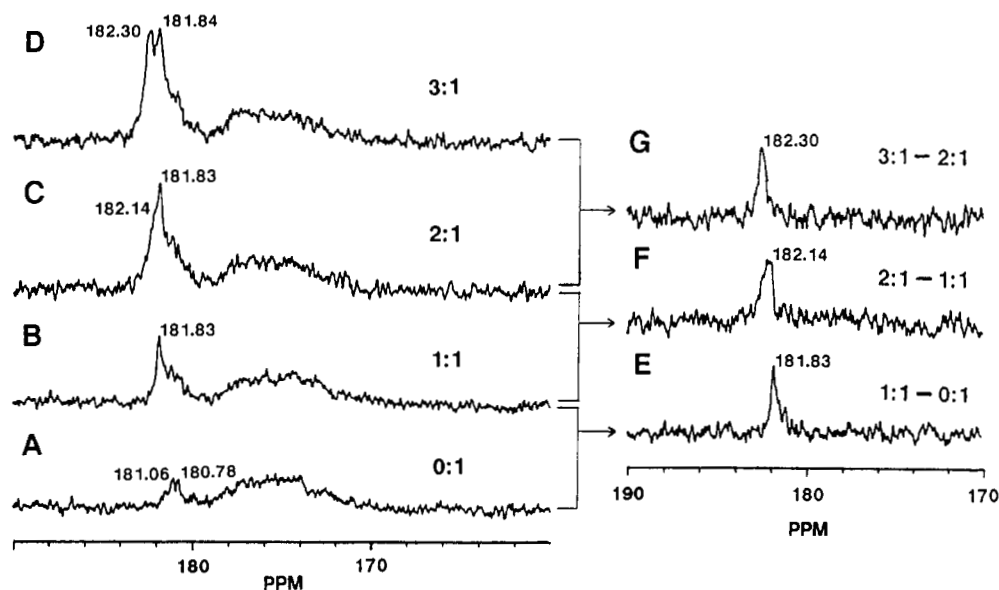


Fig. 5. The carboxyl and carbonyl regions of ^{13}C NMR spectra for 90% $[1-^{13}\text{C}]$ OCT/HSA complexes at low temperature ($T = 6.5^\circ\text{C}$), at a fixed sample pH of 7.4 ± 0.1 and at various mole ratios (A–D) with corresponding difference spectra (E–G). The spectra were recorded at a mole ratio of OCT/HSA of A) 0:1 (FA-free HSA), 3000 scans; B) 1:1, 3000 scans; C) 2:1, 2000 scans; and D) 3:1, 1186 scans. The difference spectra are displayed as follows: E) 1:1–0:1, F) 2:1–1:1, and G) 3:1–2:1 OCT/HSA. All other NMR and sample conditions were equivalent to those stated in Figs. 1 and 3.

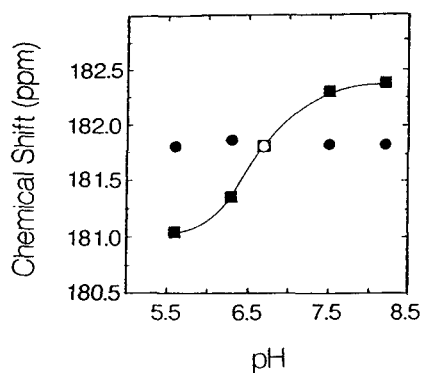


Fig. 6. Plot of the carboxyl chemical shift versus pH of the resonances for OCT in a 3:1 OCT/HSA complex at $T = 6.5^{\circ}\text{C}$. The filled circles represent the nontitrating peak at ~ 181.8 ppm and the filled squares correspond to the pH-dependent resonance. The unfilled symbol signifies overlapping chemical shift data points.

NMR studies of aqueous MCFA

The CMCs of K^+ octanoate and K^+ decanoate (400 mM and 100 mM, respectively; ref. 28) are high compared to the concentrations used in this study. Decanoic acid can form acid soap complexes at pH 7.4 at concentrations lower than 100 mM, but ^{13}C NMR signals from this phase are broad (29). Therefore, the relevant chemical shifts for comparison with data for these FA in the presence of HSA are those of the aqueous monomers. The chemical shift for OCT at a concentration equivalent to that in the 3:1 OCT/HSA mixture (6.5 mM OCT) was 184.32 ppm at 34.5°C (pH 7.4); at 6.5°C (pH 7.2) the signal shifted to 184.51 ppm. The pH dependence of the chemical shift of the carboxyl peak of aqueous OCT has been reported (19). Aqueous DEC at a concentration (6.5 mM) equivalent to a 3:1 DEC/HSA complex at pH 7.4 and 34.5°C gave a value of 184.29 ppm, nearly identical to the shift for aqueous OCT under the same experimental conditions.

Near-UV circular dichroism (CD) studies

A previous study using fluorescence-energy transfer measurements at 25°C found a very small change (<0.1 nm) in the distance between Trp-214 of HSA and bound bilirubin with the addition of up to 4 moles of OCT or DEC and a much larger change in this distance (0.2 nm) with long chain FA (30). Thus, to examine the influences of temperature and binding of MCFA on the tertiary structure of HSA, near-UV CD spectra were recorded for FA-free HSA (94 mg/ml; pH 7.4) as a function of temperature (42°C , 36°C , 25°C , 15°C , 11°C , and 7°C). No significant change in molar ellipticity as a function of temperature was seen for the HSA sample without added FA (data not shown). Further, near-UV CD spectra were recorded for a 3:1 OCT/HSA complex (pH 7.4) at protein concentrations of 94 mg/ml, 47 mg/ml, 24 mg/

ml, and 12 mg/ml and at temperatures of 42°C , 36°C , 25°C , 15°C , 11°C , and 7°C . The molar ellipticity of HSA was not changed by the presence of OCT (3:1 OCT/HSA) and this FA/HSA complex was also unaffected by temperature. A very small decrease in molar ellipticity at some wavelengths was observed upon decreasing the HSA concentration from 94 to 24 mg/ml for the 3:1 OCT/HSA mixture. Both results suggest no large conformational changes in the protein or aggregation within the temperature range examined.

DISCUSSION

Exchange of MCFA between bound and unbound pools

All NMR spectra of MCFA/HSA mixtures exhibited one or more peaks from the ^{13}C -enriched carboxyl carbon of the MCFA. These peaks occurred at chemical shifts upfield (lower ppm) from that for the aqueous MCFA in the absence of HSA and therefore reflect MCFA binding interactions with the protein. OCT/HSA complexes at 35°C (Fig. 1A) showed a single carboxyl signal whose chemical shift increased continuously as a function of mole ratio of OCT/HSA. This result is best explained by assuming rapid equilibration of bound and unbound OCT. NMR theory predicts a single, narrow peak at a chemical shift between the values for the two pools that are in fast exchange (31). The chemical shift measured for the OCT carboxyl signal in spectra of OCT/HSA mixtures would then reflect the weighted average of bound and unbound OCT. Taking the chemical shift of 184.3 ppm to represent unbound OCT and 181.8 ppm to represent bound OCT (see below), the chemical shift of 182.85 ppm at 15 mol OCT/mol HSA indicates 40% bound (or 60% unbound) OCT. The data in Fig. 1A show that the fraction of unbound OCT increases continuously with increasing mole ratio; in contrast, the fraction of unbound DEC does not become detectable until mole ratios $>12:1$.

A quantitative analysis of OCT binding to HSA was made by calculating the ratio of bound/unbound OCT from the chemical shift data in Fig. 1A and plotting these results in a Scatchard form (Fig. 1A, inset). The curve that best fits the data gave three distinct classes of binding sites with $n_1 = 2.0$ and $K_1 = 2.15 \times 10^4 \text{ M}^{-1}$; $n_2 = 5.1$ and $K_2 = 4.3 \times 10^2 \text{ M}^{-1}$; and $n_3 = 6.6$ and $K_3 = 78 \text{ M}^{-1}$. Previous studies have yielded variable predictions about the highest affinity sites on HSA for OCT. For example, Scatchard analysis has suggested $n_1 = 4.2$ and $K_1 = 6.5 \times 10^3 \text{ M}^{-1}$ (32) and $n_1 = 0.9$ and $K_1 = 2.5 \times 10^5 \text{ M}^{-1}$ with the next class of sites having $n_2 = 10$ and $K_2 = 2.7 \times 10^3 \text{ M}^{-1}$ (10). A recent study of binding of OCT to HSA by equilibrium dialysis gave a single high affinity binding site with $K_1 = 1.6 \times 10^6 \text{ M}^{-1}$ (9). An alternative treatment of binding data, the stepwise equilibrium

model, suggests that binding affinities decrease continuously as a function of added FA, i.e., the binding of the first mole of OCT occurs with $K_1 = 3.4 \times 10^4 \text{ M}^{-1}$ and the binding of each consecutive mole occurs with approximately a 3-fold lower affinity (33). Our results fall in the range of previous estimates, suggesting that our interpretation of the NMR chemical shift changes is valid. However, our analysis is limited to high ratios of OCT/HSA and cannot be used to validate or invalidate previous predictions of absolute affinities. NMR data that reflect the filling of the binding sites for OCT give unique information about relative affinities of the highest affinity binding sites (see below).

Dilution experiments provided further evidence for fast exchange between bound and unbound pools. Upon dilution of samples having fixed mole ratios of OCT/HSA, the OCT chemical shift moved to higher ppm, reflecting a higher ratio of unbound/bound OCT. Fig. 1B shows that for 10 OCT/HSA the fraction of unbound OCT was 30% for 49 mg/ml HSA and 54% for 12 mg/ml HSA. At a 3 mole ratio of OCT/HSA the fraction of unbound OCT was ~16% for 46 mg/ml HSA and ~28% for 23 mg/ml HSA. At lower OCT/HSA mole ratios, the fraction of unbound OCT will be significantly lower because the affinities of the first and second moles of OCT are much higher than that of subsequent moles (see below). As the concentration of albumin in plasma is ~50 mg/ml and the molar ratio of FA/HSA is <2 under normal conditions (34), the affinity of albumin for OCT would be sufficient for binding most of OCT (in the absence of other FA that might compete for the same binding sites).

Chemical shift data at 35°C indicated that the fraction of unbound DEC was always lower than that for OCT under comparable conditions. The data for different mole ratios of DEC/HSA at 35°C (Fig. 1A) showed a significant increase in the chemical shift of DEC only at very high mole ratios (>12/1). In dilution experiments, a measurable fraction of unbound DEC (~15%) was seen only at 10 mg HSA/ml for a 10:1 mole ratio of DEC/HSA (Fig. 1B). Our NMR approach, therefore, cannot estimate binding constants for DEC (or FA of longer chain length) because the amount of unbound FA is too low to measure reliably. However, our results do indicate that HSA has a higher affinity for DEC than OCT, in agreement with binding studies by classical methods (10, 33). In addition, previous NMR results for OCT/BSA complexes (21) show a lower fraction of unbound OCT than the present results for OCT/HSA. Therefore, HSA has a lower affinity for OCT than does BSA.

The NMR data (chemical shift and lineshape) for spectra of MCFA/HSA complexes at 35°C also provide information about the time frame of exchange. The exchange rate must be $\gg 115 \text{ sec}^{-1}$ to produce a narrow NMR signal at an intermediate chemical shift (29, 35). The average lifetime of OCT in a binding site on HSA is therefore

$< \sim 10 \text{ msec}$.² As the desorption rate of long chain FA from albumin occurs with a half-time of seconds (37), the rate of MCFA desorption from HSA is at least 10^3 times faster. This NMR result predicts that transfer of OCT from HSA to cell membranes will be very rapid and explains, at least in part, why MCFA are rapidly absorbed in patients demonstrating impaired absorption of typical long chain FA (4).

Characterization of individual binding sites

While the NMR data at temperatures close to physiological temperature provided important information about MCFA equilibration between HSA and the aqueous phase, they did not provide molecular details of binding sites on HSA. To pursue such information, we focused on low MCFA/HSA mole ratios, where the highest affinity binding site(s) can be observed (and the unbound pool of MCFA will be the lowest), and on low temperature, as the affinity of OCT and DEC for HSA is 2–3 times higher at 5°C than at 25°C (10). At ~6°C, multiple NMR signals were seen for OCT/HSA and DEC/HSA mixtures (Figs. 3, 4, and 5) at chemical shifts very similar to those shifts for longer chain (≥ 12 carbons) FA bound to HSA (see results and ref. 26) or BSA (16, 18) and for OCT and DEC complexes with BSA (21). This close correspondence of chemical shifts argues for similar types of interactions of the carboxyl groups of medium and long chain FA with HSA.³

General similarities in binding of medium- and long-chain fatty acids are also suggested from titration data at 6°C (Fig. 6), showing an insensitivity of chemical shift to pH. The carboxylate of OCT in its two highest affinity sites may be stabilized by salt bridges with basic amino acid(s) which depress the pKa of the FA carboxylate, as shown for longer chain FA in high affinity sites (16, 19). In the X-ray crystallographic structure of HSA, binding sites for an aromatic acid were observed in domains IIa and IIIa; the carboxylate was stabilized by basic amino acid residues in both sites (2). Data from numerous earlier studies have suggested localization of binding sites for MCFA in these domains (3).

²It is interesting to note that a recent NMR study of binding of a fluorinated anesthetic, isoflurane, to BSA revealed fast exchange of bound and unbound ligand. The off rate constant was $\sim 4000 \text{ s}^{-1}$ (36), and the dissociation constant ($K_D = 1.4 \text{ mM}$) was somewhat higher than that derived from our data ($1/K_1 = 50 \text{ } \mu\text{M}$) for OCT.

³The binding sites or binding interactions are not necessarily identical for different FA, even when the chemical shifts are identical, as the chemical shift represents the net magnetic environment of the nucleus; the individual components are not known. Previous data (3) suggest that one binding site for OCT may be unique and other sites may be the same as those for long-chain FA. Competition experiments with an NMR approach suggest one unique binding site for OCT on HSA (M. A. Kenyon and J. A. Hamilton, unpublished results). Given the close similarity of chemical shifts of MCFA and long-chain FA bound to albumin, a correspondence of other binding sites is possible.

The temperature-dependent spectra of OCT (and DEC) complexes with HSA at a 3/1 mole ratio (Figs. 3 and 4) are characteristic of an exchange process: a single, narrow signal broadens, becomes asymmetric, and splits into multiple narrow signals with decreasing exchange rate. As a quantitative test of this interpretation of these spectroscopic changes, we calculated exchange rates of 36.5 sec^{-1} at 11.5°C and 102.8 sec^{-1} at 16°C (21, 35), corresponding to mean lifetimes (τ) of 27 msec and 9.7 msec, respectively. These rates are consistent with the finding that exchange at 35°C between bound and unbound pools of OCT occurs at a rate of $>115 \text{ sec}^{-1}$ ($\tau < 10$ msec). Therefore, we conclude that the exchange rate of OCT between binding sites is slow on the NMR chemical shift time scale at 6°C , as is the case for OCT binding to BSA (21), giving rise to separate signals. At 35°C exchange between binding sites is rapid, obscuring the interactions in individual sites. Similar arguments hold for binding of DEC to HSA, although the temperature-dependent spectra for DEC were not amenable to quantitative analysis. Exchange of DEC between binding sites on BSA occurred about 10 times slower than that for OCT (21); a similar difference would be expected for HSA.

In addition to exchange of MCFA between binding sites, changes in protein tertiary structure with temperature could influence the carboxyl chemical shift of MCFA bound to HSA. However, the near-UV CD results revealed no major conformational changes in the tertiary structure of HSA within the temperature range where the NMR lineshape changes were seen. Furthermore, complexes of lauric acid with HSA showed identical, multiple carboxyl resonances at both low and high temperatures, suggesting no major conformational changes due to temperature and/or aggregation. It is still possible that small undetected temperature-dependent tertiary structural changes make a minor contribution to chemical shift changes for MCFA that are superimposed on larger changes from exchange.

With the capability of differentiating binding sites at low temperature, it was possible to determine the relative⁴ affinities for the first three binding sites on HSA for OCT. Difference spectra (Fig. 5) showed a single peak⁵ for OCT after the first, second, and third moles of OCT were added to HSA, showing that the affinities for each successive site differ by at least a factor of five, based on the

⁴It must be emphasized that NMR data obtained under the conditions where the multiple sites are observed (low temperature and low mole ratios) do not detect unbound OCT and thus do not give absolute affinity constants.

⁵As discussed above, an NMR signal at a specific chemical shift can represent more than one binding site, even with exchange processes eliminated. Here we take the simplest interpretation that each well-differentiated peak represents a single binding site, which is reasonable because of the stoichiometric relationship seen in Fig. 5.

signal-to-noise ratios in the spectra. Therefore, the two high affinity sites with apparently equal affinities determined from our Scatchard plot (Fig. 1A) are differentiated by NMR. The sequential filling of binding sites on albumin by OCT contrasts with the simultaneous filling by long-chain FA of binding sites on both BSA (16, 18) and HSA (26). In contrast, the stepwise equilibration analysis (33) does not predict significant differences in relative affinities of HSA for the first three moles of OCT or for the first three moles of longer chain FA.

A surprising finding was that the primary binding site for OCT and DEC on HSA gave rise to NMR signals at distinctly different chemical shifts (181.8 ppm for OCT and 182.3 ppm for DEC). The chemical shift of each was independent of pH and temperature. As aqueous (unbound) OCT and DEC both give a signal at 184.3 ppm, OCT and DEC must bind to two different sites on HSA or to the same site but with different interactions within this site. NMR studies in which both FA competed for binding to HSA suggest that the sites for OCT and DEC are distinct (M. A. Kenyon and J. A. Hamilton, unpublished results). It was also interesting that the NMR signal for the third mole of OCT added to HSA gave a signal at the same chemical shift for the first mole of DEC (182.3 ppm). Whether these are the same sites is difficult to assess because the identity of chemical shift does not necessarily indicate an identity of a particular binding site or of its interactions.³ Studies with MCFA containing enrichment in different carbons could resolve these ambiguities by showing differences or similarities within the binding sites (38). ■

The authors wish to acknowledge Dr. Mary Walsh for assistance with the CD measurements and Margaret Gibbons for preparation of the manuscript. This research was supported by United States Public Health Services Grant HL-26335.

Manuscript received 30 May 1993 and in revised form 27 September 1993.

REFERENCES

1. Spector, A. A., and J. E. Fletcher. 1982. Transport of fatty acid in circulation. In *Disturbances in Lipid and Lipoprotein Metabolism*. J. M. Dietschy, A. M. Gotto, Jr., and J. A. Ontko, editors. American Physiological Society, Bethesda, MD. 229-249.
2. He, X.-M., and D. C. Carter. 1992. Atomic structure and chemistry of human serum albumin. *Nature*. **358**: 209-215.
3. Brown, J. R., and P. Shockley. 1982. Serum albumin: structure and characterization of its ligand binding site. In *Lipid Protein Interactions*. P. C. Jost and O. H. Griffith, editors. Wiley, NY. 26-68.
4. Bach, A. C., and V. K. Babayan. 1982. Medium-chain triglycerides: an update. *Am. J. Clin. Nutr.* **36**: 950-962.
5. Babayan, V. K. 1987. Medium chain triglycerides and structured lipids. *Lipids*. **22**: 417-420.
6. Greenberger, N. J., and T. G. Skillman. 1969. Medium chain triglycerides: physiological considerations and clinical

- implications. *N. Engl. J. Med.* **280**: 1045-1058.
7. Bougnères, P. F., L. Castaño, F. Rocchiccioli, H. Pham Gia, B. Leluyer, and P. Ferre. 1989. Medium-chain fatty acids increase glucose production in normal and low birth weight newborns. *Am. J. Physiol.* **256**: E692-E697.
 8. Kragh-Hansen, U. 1981. Molecular aspects of ligand binding to serum albumin. *Pharmacol. Rev.* **33**: 17-53.
 9. Kragh-Hansen, U. 1991. Octanoate binding to the indole and benzodiazepine-binding region of human serum albumin. *Biochem. J.* **273**: 641-644.
 10. Lee, I. Y., and R. H. McMenamy. 1980. Location of the medium chain fatty acid site on human serum albumin. *J. Biol. Chem.* **255**: 6121-6127.
 11. Cunningham, V. J., L. Hay, and H. B. Stoner. 1975. The binding of L-tryptophan to serum albumins in the presence of nonesterified fatty acids. *Biochem. J.* **146**: 653-658.
 12. Ashbrook, J. D., A. A. Spector, and J. E. Fletcher. 1972. Medium chain fatty acid binding to human plasma albumin. *J. Biol. Chem.* **247**: 7038-7042.
 13. Koh, S-W., and G. E. Means. 1979. Characterization of a small apolar anion binding site of human serum albumin. *Arch. Biochem. Biophys.* **192**: 73-79.
 14. King, T. P. 1973. Limited pepsin digestion of bovine plasma albumin. *Arch. Biochem. Biophys.* **156**: 509-520.
 15. Reed, R. G., R. C. Feldoff, and T. Peters, Jr. 1976. Fragments of bovine serum albumin produced by limited proteolysis: complementary behavior of two large fragments. *Biochemistry.* **15**: 5394-5398.
 16. Parks, J. S., D. P. Cistola, D. M. Small, and J. A. Hamilton. 1983. Interactions of the carboxyl group of oleic acid with bovine serum albumin: a ^{13}C NMR study. *J. Biol. Chem.* **258**: 9262-9269.
 17. Hamilton, J. A., and D. P. Cistola. 1986. Transfer of oleic acid between albumin and phospholipid vesicles. *Proc. Natl. Acad. Sci. USA.* **83**: 82-86.
 18. Cistola, D. P., D. M. Small, and J. A. Hamilton. 1987. Carbon 13 NMR studies of saturated fatty acids bound to bovine serum albumin. I. The filling of individual fatty acid binding sites. *J. Biol. Chem.* **262**: 10971-10979.
 19. Cistola, D. P., D. M. Small, and J. A. Hamilton. 1987. Carbon 13 NMR studies of saturated fatty acids bound to bovine serum albumin. II. Electrostatic interactions in individual fatty acid binding sites. *J. Biol. Chem.* **262**: 10980-10985.
 20. Hamilton, J. A., S. Era, S. P. Bhamidipati, and R. G. Reed. 1991. Locations of the three primary binding sites for long chain fatty acids on bovine serum albumin. *Proc. Natl. Acad. Sci. USA.* **88**: 2051-2054.
 21. Hamilton, J. A. 1989. Medium-chain fatty acid binding to albumin and transfer to phospholipid bilayers. *Proc. Natl. Acad. Sci. USA.* **86**: 2663-2667.
 22. Janatova, J., J. K. Fuller, and M. J. Hunter. 1968. The heterogeneity of bovine albumin with respect to sulfhydryl and dimer content. *J. Biol. Chem.* **243**: 3612-3622.
 23. Beaven, G. H., S. H. Chen, A. D'Albis, and W. B. Gratzer. 1974. A spectroscopic study of the haemin-human serum-albumin system. *Eur. J. Biochem.* **41**: 539-546.
 24. Levy, G. C., and I. R. Peat. 1975. The experimental approach to accurate carbon-13 spin-lattice relaxation measurements. *J. Magn. Reson.* **18**: 500-521.
 25. Greenfield, N., and G. D. Fasman. 1969. Computed circular dichroism spectra for the evaluation of protein conformation. *Biochemistry.* **8**: 4108-4116.
 26. Cistola, D. P. 1985. Physicochemical studies of fatty acids in model biological systems. Ph.D. Dissertation. Boston University School of Medicine.
 27. Cistola, D. P., D. M. Small, and J. A. Hamilton. 1982. Ionization behavior of aqueous short-chain carboxylic acids: a carbon-13 NMR study. *J. Lipid Res.* **23**: 795-799.
 28. Mukerjee, P., and K. J. Mysels. 1971. Critical Micelle Concentration of Aqueous Surfactant Systems. National Bureau of Standards, Washington, DC.
 29. Cistola, D. P., J. A. Hamilton, D. Jackson, and D. M. Small. 1988. Ionization and phase behavior of fatty acids in water: application of the Gibbs phase rule. *Biochemistry.* **27**: 1881-1888.
 30. Honoré, B., and A. O. Pederson. 1989. Conformational changes in human serum albumin studied by fluorescence and absorption spectroscopy. *Biochem. J.* **258**: 199-204.
 31. Shaw, D. 1976. Fourier Transform NMR Spectroscopy. Elsevier Scientific Publishing, Amsterdam. 231-233.
 32. Teresi, J. D., and J. M. Luck. 1952. The combination of organic anions with serum albumin. VIII. Fatty acid salts. *J. Biol. Chem.* **194**: 823-834.
 33. Spector, A. A. 1975. Fatty acid binding to plasma albumin. *J. Lipid Res.* **16**: 165-179.
 34. Spector, A. A. 1986. Plasma albumin as a lipoprotein. In *Biochemistry and Biology of Plasma Lipoproteins*. A. M. Scanu and A. A. Spector, editors. Marcel Dekker, New York. 247-279.
 35. Roberts, J. K. M., and O. Jardetzky. 1985. Nuclear magnetic resonance spectroscopy in biochemistry. In *Modern Physical Methods in Biochemistry*. Neuberger and van Deenen, editors. Elsevier Science Publishers, New York. 1-67.
 36. Dubois, B. W., and A. S. Evers. 1992. ^{19}F -NMR spin-spin relaxation (T_2) method for characterizing volatile anesthetic binding to proteins. Analysis of isoturane binding to serum albumin. *Biochemistry.* **31**: 7069-7076.
 37. Daniels, C., N. Noy, and D. Zakim. 1985. Rates of hydration of fatty acids bound to unilamellar vesicles of phosphatidylcholine or to albumin. *Biochemistry.* **24**: 3286-3292.
 38. Hamilton, J. A., D. P. Cistola, J. D. Morrisett, J. T. Sparrow, and D. M. Small. 1984. Interactions of myristic acid with bovine serum albumin: a ^{13}C NMR study. *Proc. Natl. Acad. Sci. USA.* **81**: 3718-3722.